Molecular Therapy
Oncolytics
Original Article

Endogenous H3.3K27M derived peptide restricted to HLA-A*02:01 is insufficient for immune-targeting in diffuse midline glioma

Stacie S. Wang,[1,2,3,7] Kirti Pandey,[4,7] Katherine A. Watson,[1] Rebecca C. Abbott,[1,3] Nicole A. Mifsud,[4] Fiona M. Gracey,[5] Sri H. Ramarathinam,[4] Ryan S. Cross,[1,7] Anthony W. Purcell,[4,7] and Misty R. Jenkins[1,3,6,7]

[1]The Walter and Eliza Hall Institute of Medical Research, Immunology Division, Parkville, VIC 3052, Australia; [2]Murdoch Children's Research Institute, Parkville, VIC 3052, Australia; [3]The University of Melbourne, Department of Medical Biology, Parkville, VIC 3052, Australia; [4]Department of Biochemistry and Molecular Biology and Infection and Immunity Program, Biomedicine Discovery Institute, Monash University, Clayton, VIC 3800, Australia; [5]Myrio Therapeutics, 6-16 Joseph St, Blackburn North, Melbourne, VIC 3130, Australia; [6]La Trobe University, La Trobe Institute for Molecular Science, Bundoora, VIC, Australia

Diffuse midline glioma (DMG) is a childhood brain tumor with an extremely poor prognosis. Chimeric antigen receptor (CAR) T cell therapy has recently demonstrated some success in DMG, but there may a need to target multiple tumor-specific targets to avoid antigen escape. We developed a second-generation CAR targeting an HLA-A*02:01 restricted histone 3K27M epitope in DMG, the target of previous peptide vaccination and T cell receptor-mimics. These CAR T cells demonstrated specific, titratable, binding to cells pulsed with the H3.3K27M peptide. However, we were unable to observe scFv binding, CAR T cell activation, or cytotoxic function against H3.3K27M^{+} patient-derived models. Despite using sensitive immunopeptidomics, we could not detect the H3.3K27M$_{26–35}$-HLA-A*02:01 peptide on these patient-derived models. Interestingly, other non-mutated peptides from DMG were detected bound to HLA-A*02:01 and other class I molecules, including a novel HLA-A3-restricted peptide encompassing the K27M mutation and overlapping with the H3 K27M$_{26–35}$-HLA-A*02:01 peptide. These results suggest that targeting the H3 K27M$_{26–35}$ mutation in context of HLA-A*02:01 may not be a feasible immunotherapy strategy because of its lack of presentation. These findings should inform future investigations and clinical trials in DMG.

INTRODUCTION

Uncommon and low survival cancers necessitate innovative strategies. Diffuse midline gliomas (DMGs), of which diffuse intrinsic pontine glioma (DIPG) is a subtype, are rare and fatal childhood brain tumors.[1] Three significant studies[2–4] identified a recurrent driver mutation in histone 3 variants 1 and 3 (H3.1, H3.3) resulting in a replacement of lysine by methionine at position 27 (K27M) in 70%–80% of DMG tumors. This mutation disrupts lysine methyltransferases binding sites, altering the tumor's epigenetic landscape[3] and potentially contributing to poorer prognosis in both H3.1 and H3.3 tumors.[5] The H3.3K27M mutation has been reported to create a peptide (H3.3K27M$_{26–35}$, RMSAPSTGGV), predicted to bind to human leukocyte antigen (HLA)-A*02:01 anchored through the methionine mutation with high affinity (NetMHC v3.4: 285 nM). Conversely, the wild-type (WT) peptide (H3.3$_{26–35}$) is not predicted to bind to HLA-A*02:01.[6] Experimental validation by Chhedda et al.[6] had confirmed the high affinity binding of this peptide to HLA-A*02:01 using a competitive inhibition assay.

Targeting driver mutations, such as H3.3K27M, presented on cell surfaces as HLA-bound peptides (pHLAs), holds promise for cancer specific immunotherapies, including vaccination and adoptive cell therapies like T cell receptor (TCR)-like or chimeric antigen receptor (CAR)-based approaches. Success in targeting neoepitope driver mutations, like KRASG12D-HLA-C*08:02 in pancreatic cancer, highlights the potential of such strategies.[7] Tumors like H3.3K27M-HLA-A*02:01^{+} DMG are the ideal candidates for immunotherapeutic options. However, in addition to the target being a driver of disease, it must also be represented within the immunopeptidome at the tumor cell surface.

The H3.3K27M$_{26–35}$ peptide has been the focus of immune vaccine and TCR mimic strategies,[6,8] with a clinical trial underway for newly diagnosed H3.3K27M positive DMG patients who are HLA-A*02 positive.[8] Further, several clinical trials have been announced or are actively recruiting HLA-A*02:01^{+} patients with H3.3K27M mutated glioma including; ENACTING trial using an H3.3K27M peptide (*NCT04749641*), and PNOC018 trial using genetically modified KIND T cells (*NCT05478837*).

We have previously described the characterization of a novel H3.3K27M-HLA-A*02:01 specific CAR and shown a functional

Received 1 May 2023; accepted 11 August 2023;
https://doi.org/10.1016/j.omto.2023.08.005.

[7]These authors contributed equally

Correspondence: Misty R. Jenkins, The Walter and Eliza Hall Institute of Medical Research, Immunology Division, Parkville, VIC 3052, Australia.
E-mail: jenkins.m@wehi.edu.au

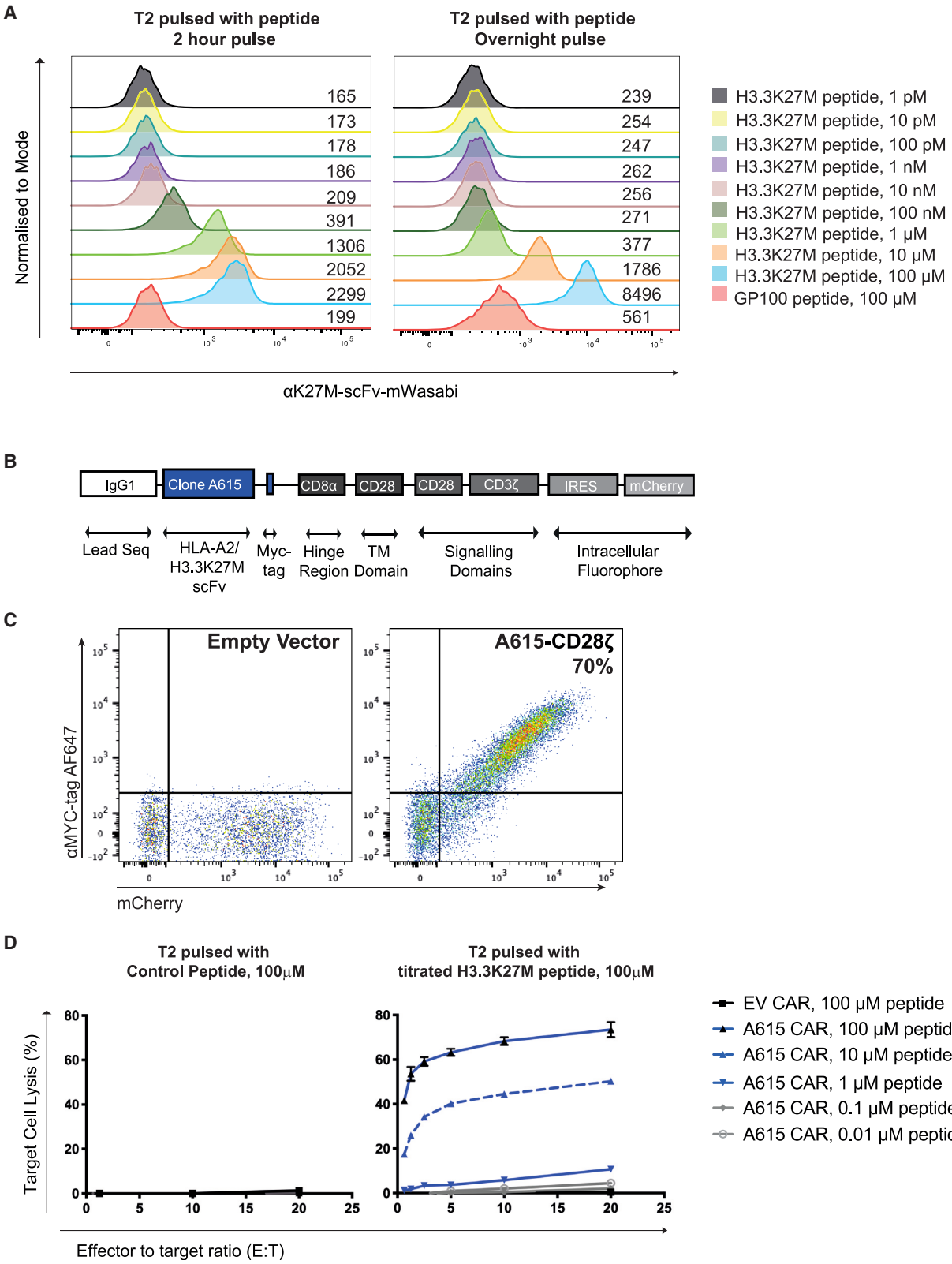

(legend on next page)

immune synapse, characteristic of a classical TCR-like immune synapse structure.[9] In this study, we present the characterization of a novel single chain variable fragment (scFv) domain, named A615, targeting H3.3K27M-HLA-A*02:01, which we engineered into second generation CD28ζ CARs.

The CAR approach offers distinct therapeutic advantages compared to peptide vaccination or a TCR-based approach. It enables the redirection of both $CD4^+$ and $CD8^+$ T cells using a single receptor. Furthermore, the affinity of the scFv can be fine-tuned or selected for higher affinity to the H3.3K27M-HLA-A*02:01 peptide-major histocompatibility complex (MHC) complex. This feature helps overcome limitations with the natural TCR repertoire and has potential to reduce the risk of on-target, off-tumor effects.

In this study, we show that H3.3K27M-HLA-A*02:01 directed CAR T cells are functional, recognizing H3.3K27$M_{26–35}$ peptide loaded TAP-deficient antigen-presenting cells (APC). However, when our H3.3K27M-HLA-A*02:01 CAR T cells were co-cultured with endogenous H3.3K27M-HLA-A*02:01^+ DMG patient-derived models, they failed to elicit any functional responses. We used mass spectrometry to definitively show that the H3.3K27M-derived mutant peptide is not endogenously presented by HLA-A*02:01 across multiple DMG cell lines, while demonstrating that an HLA-A*03:01-mutant-derived peptide can be presented at the cell surface. The H3.3K27M-HLA-A*02:01 peptide-MHC complex is not an effective target for cancer immunotherapy because of the lack of antigen density at the cell surface.

RESULTS

H3.3K27M-HLA-A*02 targeting scFv and CAR T constructs recognize peptide pulsed APC

In our previous work, we developed a scFv antibody that targets the novel H3.3K27M-HLA-A*02:01 peptide-MHC complex.[9] Among the reactive scFv reactive clones, we identified the most effective one, named A615, for further investigation.[9] The A615 scFv was then engineered with an avitag, allowing the production of A615-tetramer-mWasabi conjugates for easy detection using flow cytometry. Using this A615-tetramer-mWasabi, we examined the peptide concentration and peptide retention dynamics of the H3.3K27M-HLA-A*02:01 complex on TAP deficient HLA-A*02:01^+ T2 target cells (Figure 1A).

In our experiments, we first assessed the binding of the A615 tetramer to T2 cells pulsed with titrated concentrations of the H3.3K27$M_{26–35}$ peptide (Figure 1A). We found that the A615 tetramer could detect peptide-pulsed H3.3K27M-HLA-A*02:01 complex down to 100 nM. However, to maintain A615 tetramer detection overnight, a minimum of 10 μM of H3.3K27M peptide was required, while lower concentrations did not sustain detection.

Next, we incorporated the A615 scFv clone into a second-generation CAR, which included an MYC-tag in the hinge and CD28-CD3 ζ signaling tail, along with an IRES mCherry reporter (Figure 1B). We observed robust cell surface expression of the A615 CAR, as demonstrated by detection of the MYC-tag, and correlating with mCherry expression levels (Figure 1C).

To investigate whether tetramer staining of peptide-pulsed cells correlated with CAR T cell function, we conducted a short-term 4-h chromium killing assay (Figure 1D). A615 CAR T cells exhibited specific cytotoxicity against T2 cells pulsed with the H3.3K27M peptide across broad E:T ratios (20:1 to 1.25:1). However, the killing efficiency was reduced at peptide concentrations between 10 μM and 1 μM across all ratios. These findings aligned with the limits of detection observed with the A615 tetramer by flow cytometry, establishing a correlation between tetramer flow cytometry detection and CAR T cell function.

H3.3K27M-HLA-A2 targeting scFv and CAR T constructs fail to recognize H3.3K27M-mutated DIPG cell lines

Having verified the specificity and functionality of both A615-tetramer and A615 CAR T cells, our next objective was to assess their effectiveness against patient derived models. We screened a selection of H3.3K27M DIPG cell lines to identify those expressing HLA-A*02 on the cell surface using flow cytometry and immunogenetics. Among the DIPG cell lines examined, SU DIPG 27, 35, 38, and 43 through immunogenetics were found to be HLA-A*02:01^+ (listed in Table S1), as well as HSJD DIPG 17 and HSJD DIPG 21, SU DIPG 35 and SU DIPG 43 were shown to be HLA-A*02^+ by flow cytometry (Figure 2A).

To evaluate the functionality of the A615 CAR, we tested A615-tetramer binding against four of the models, including HSJD DIPG 17, 21, and SU DIPG 35, 43. Interestingly, no binding of A615 tetramer was observed with any DIPG cell lines examined (Figure 2B). To further explore the lack of recognition by A615 CAR T cells we conducted additional experiments. We exposed four H3K27M-HLA-A*02:01 DIPG cell lines (SU DIPG 35, SU DIPG 43, HSJD 17, and HSJD 21) to 100 μM H3.3K27M peptide at 37°C for 2 h, before interrogation with A615-tetramer (Figure 2B). The results showed a detectable increase in H3.3K27M-HLA-A*02:01 binding as indicated by increases in mean fluorescence intensity (MFI) for

Figure 1. Binding and functional recognition of peptide pulsed APC by H3.3K27M-HLA-A*02:01 specific A615 constructs

(A) Flow cytometry histograms displaying tetrameric A615 scFv-mWasabi binding to the H3.3K27M-HLA-A*02:01 peptide MHC complex on T2 cells peptide pulsed for 2 h or overnight. MFI denoted to the right of flow peaks. Data are representative of two experiments. (B) Construct schematic of the second generation A615 anti- H3.3K27M-HLA-A*02:01 CAR containing CD28ζ co-stimulation domain. (C) Flow cytometry of C57Bl/6 $CD8^+$ CAR T cell CAR expression. Shown is mCherry and MYCtag expression by empty vector or A615 expressing CAR T cells. (D) Cytotoxic capacity of C57Bl/6 $CD8^+$ A615 CAR T cells as assayed by 4 h co-culture with chromium-labeled T2 cells pulsed with titrated concentrations of H3.3K27$M_{26–35}$ peptide. The empty vector (EV) CAR is provided as a negative control. Shown is the mean 4 h percentage of maximum target cell lysis in triplicate ± SD. Data are representative of two biological replicates.

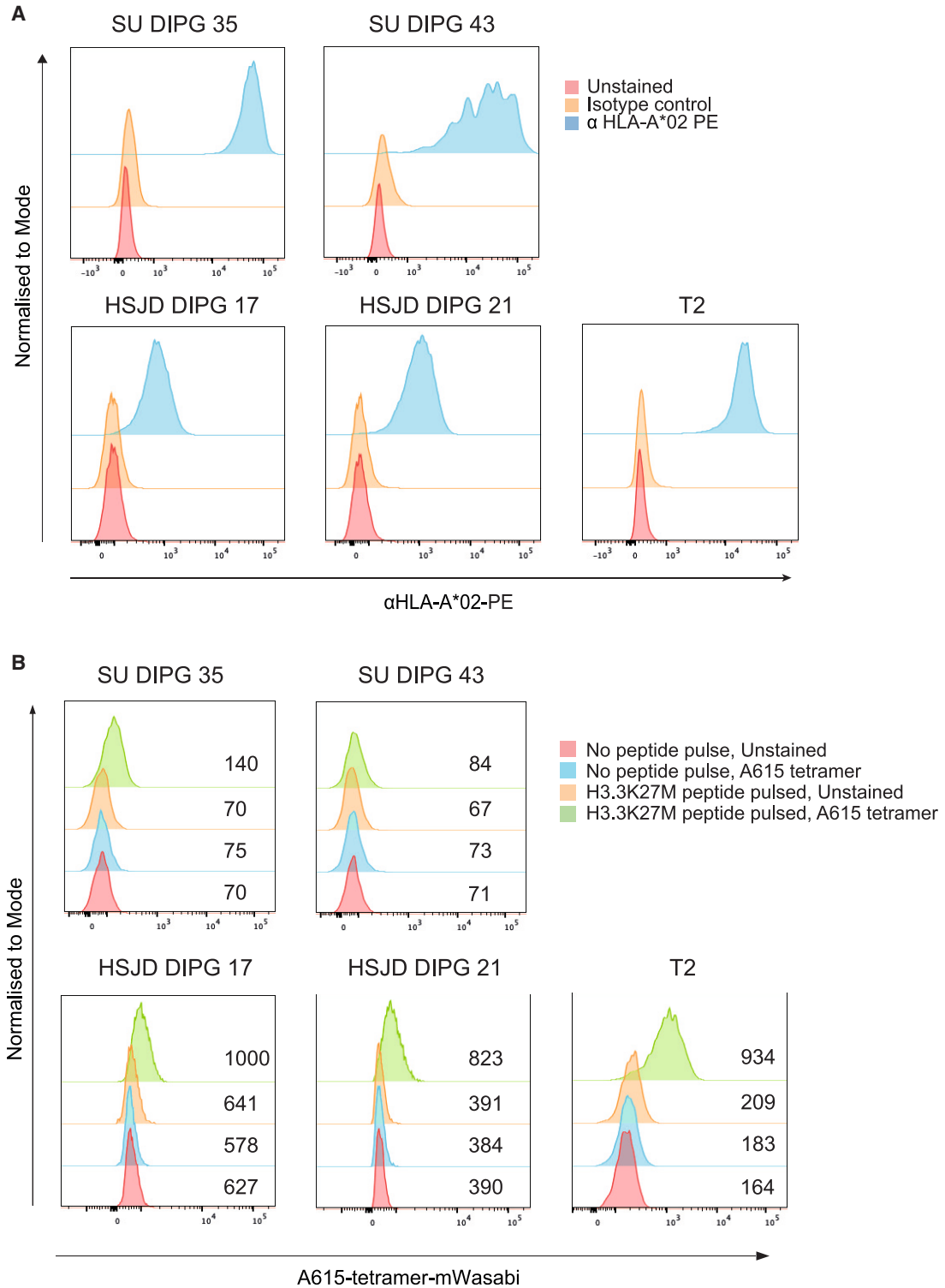

Figure 2. Flow cytometry analysis demonstrates that DIPG patient derived cells are HLA-A2^{+} but that H3.3K27M-HLA-A*02:01 is not endogenously detected at the cell surface

(A) Flow cytometry histograms displaying HLA-A-2*02-PE binding to different patient derived DIPG cell lines and T2 cells. (B) Flow cytometry histograms displaying tetrameric A615 scFv-488 binding to the H3.3K27M-HLA-A*02:01 peptide MHC complex of most HLA-A2 positive, DIPG cells when H3K27M$_{26–35}$ peptide pulsed, but not SU DIPG 43. MFI denoted to the right of flow peaks. Data are representative of two experiments.

SU DIPG 35, HSJD 17 and HSJD 21 after peptide pulsing, but not for SU DIPG 43, which carries the H3.1K27M mutation.

To address the possibility that the level of H3.3K27M peptide binding to HLA-A*02:01 might be too low to be detected by flow cytometry, we took into consideration that even very minimal antigen presentation could potentially activate CAR T cells. Therefore, we conducted further investigations to determine whether the A615 CAR T cells could effectively eliminate the three H3.3K27M-HLA-A*02:01$^+$ DIPG cell lines that showed detectable labeling with the H3.3K27M peptide.

On day 8, effector A615 CAR T cells were co-cultured with both DIPG and T2 target cells, where the latter were either pulsed with H3.3K27M peptide (at 100 μM) or left unpulsed. As another negative control, non-specific G100 peptide was pulsed on T2 cells to stabilize cell surface HLA-A2. To assess cytotoxicity, the cells were labeled with chromium and cultured for 4 h, after which the percentage target cell lysis was determined based on chromium release measurements in the supernatant.

The results showed that the A615 CAR T cells exhibited significant cytotoxicity against T2 targets that were pulsed with H3.3K27M peptide, but not G100 (Figure 3), indicating their ability to specifically recognize and kill H3.3K27M peptide-loaded targets.

However, it is noteworthy that no cytotoxic response was observed when A615 CART cells were cultured with any of the DIPG lines, regardless of whether the DIPG cells were pulsed with the H3.3K27M peptide or left unpulsed (Figure 3). This indicates that the A615 CAR T cells did not demonstrate a cytotoxic effect against the DIPG cell lines under the conditions tested.

The H3.3K27M peptide is not endogenously presented in HLA-A*02:01$^+$ DIPG cell lines

To understand why our H3.3K27M-HLA-A*02:01-specific A615 CAR T cells and A615-tetramer did not detect endogenous H3.3K27M-HLA-A*02:01, we conducted immunoaffinity purification to capture HLA-A*02:01-bound peptides and immunopeptidomics to confirm the presentation of this peptide in the MHC complex. In this discovery-based approach, we characterized the repertoire of peptides presented by HLA-A*02:01$^+$ H3.3K27M-mutated DIPG cell lines, including SU DIPG 27, SU DIPG 35, SU DIPG 38, and the H3.1K27M-mutated SU DIPG 43 model (Table S1).

Surprisingly, we did not detect the H3.3K27M peptide (RMSAP STGGV)[6] within these HLA-A*02:01$^+$ cell line models (Table S2). Instead, we found the elution of 11 WT histone 3 peptides from HLA-A*02, with 8 of them annotated in IEDB and 4 being conserved across all cell lines examined. These data demonstrate that histone 3.3 is undergoing proteasomal degradation, and the liberated peptide antigens are presented at the cell surface.

To further investigate the lack of detection of the H3.3K27M peptide, we developed more sensitive multiple reaction monitoring (MRM) assays for peptide identification. After elution, samples were spiked with an internal heavy peptide standard that co-elutes with any endogenous "light" peptide, but differs by the introduced 6-Da mass increase, enabling confident identification of the endogenous peptide. In the study by Chheda et al..,[6] only an oxidized species of this peptide was detected (MetOx at P2). A total of 24 MRM transitions were selected, including both native (RMSAPSTGGV) and modified peptides (RM_{ox}-SAPSTGGV), both heavy and endogenous peptide versions (Table S3). Alongside, MRM transitions were also established for six constitutively presented HLA-A*02:01 restricted peptides including TLADLVHHV, ATYVFLHTV, VMDSKIVQV, YLGRLAHEV, RMLPHAPGV, and VLYDQPRHV.

We examined the HLA-A2 (clone BB7.2) eluates of SU DIPG 27, 35, 38, and 43 using these MRM assays (Figures 4A–4D). While the heavy labeled internal peptide standard was identified in all samples, the endogenous neoepitope (RMSAPSTGGV) was not detected in any of the cell lines either as the native or oxidized species. In contrast, we identified all six constitutive HLA-A*02:01 control peptides in SU DIPG35 and SU DIPG 38, while only four were identified in SU DIPG 43 (Figure S1).

Since we could not detect the H3.3K27M peptide on the endogenous DIPG cell lines, we decided to explore peptide presentation after pulsing these cells with the H3.3K27M peptide. The goal was to determine whether this peptide could be presented in association with HLA-A*02:01.

To achieve this, we performed a peptide elution following peptide pulsing HSJD DIPG 21 cells, as they exhibited the most significant MFI shift when exposed to the peptide (Figure 2B). Additionally, we conducted experiments using T2 cells, where we titrated HLA-A*02:01 peptides, and then used MRM-HR to detect peptide presentation.

In the HSJD DIPG 21 cells, no detectable endogenous peptide presentation was observed (Figure 4E). However, when these cells were pulsed with 100 μM H3.3K27M peptide, a peak corresponding with H3K27M presentation was evident. This peak was lower in intensity compared to the 100 μM peak observed in T2 cells but was greater than the peak seen in T2 cells pulsed with 10 μM K27M peptide, which was also included in the examination. Collectively, these data demonstrate a lack of detectable endogenous H3.3K27M peptide presentation in HLA-A2*02:01 DIPG cells. However, the results indicate that H3.3K27M peptide can be presented in association with HLA-A02:01 upon exogenous loading of some HLA-A*02$^+$ cells, including HSJD DIPG21 cells, but not at a level that resulted in A615 CAR T cell cytotoxicity (Figure 3).

We discovered presentation of a novel HLA-A*03:01 restricted neopeptide and non-mutated H3.3-derived peptides

Since we could not detect the HLA-A2 neopeptide in the DIPG cell lines, we turned our attention to an alternate HLA-A*02:01-positive cell line, HEK293T (Table S1). To ensure high-level expression of the mutant protein, we transfected the HEK293T cells with a plasmid encoding the H3.3K27M histone. The HEK293T parental (WT) cells are known to have high HLA class I expression.[10] We then used

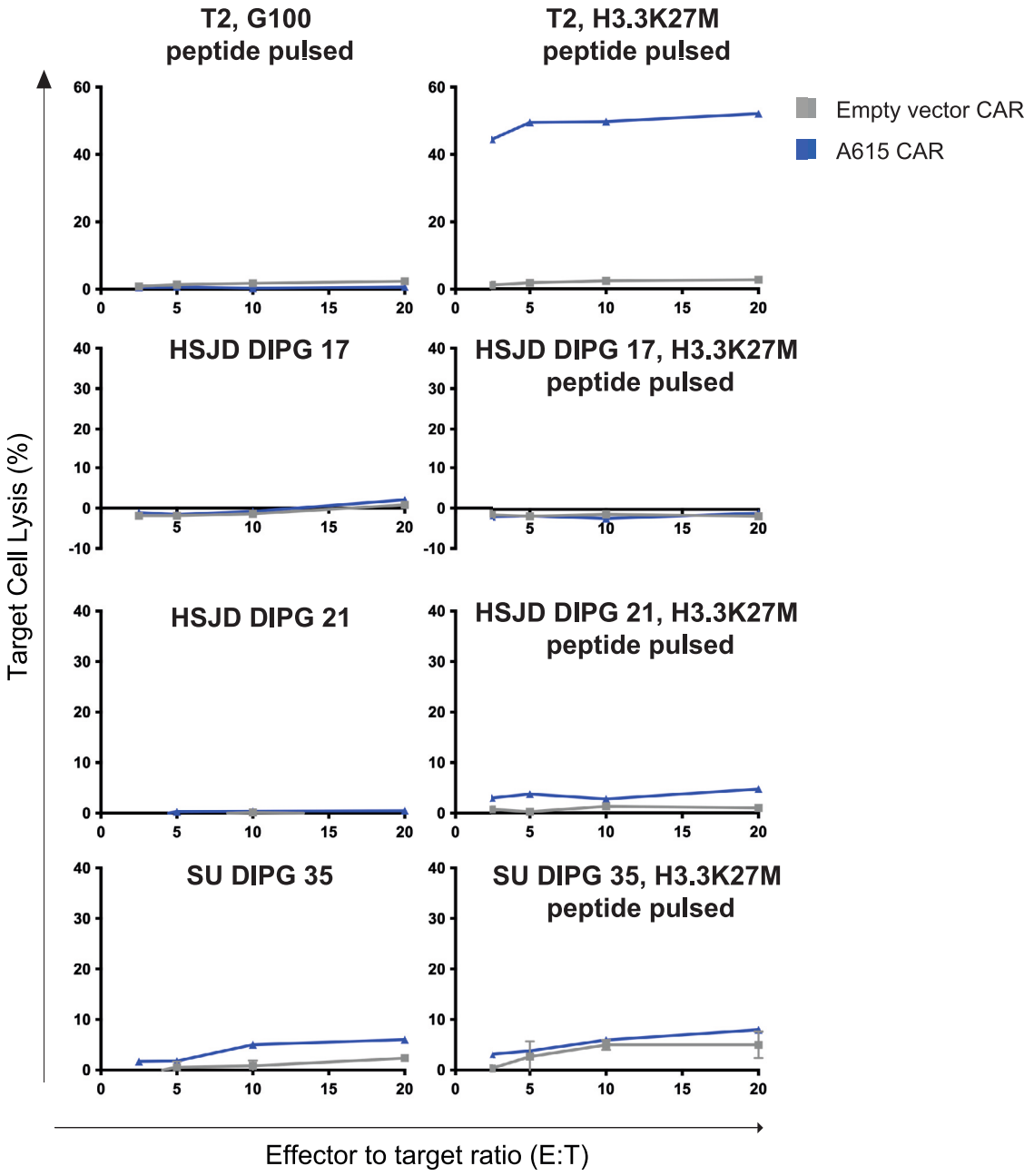

Figure 3. Cytotoxic interrogation of the A615 CAR against H3.3K27M$_{26–35}$ peptide pulsed and H3.3K27M endogenous DIPG cell lines in a chromium release assay
The cytotoxic capacity of A615 CAR T cells (blue lines) as assayed by 4 h co-culture with chromium labeled target cells. Day 8 after activation C57Bl/6 CD8$^+$ CAR T cells were cultured with 3 HLA-A*02 positive DIPG lines, by themselves or pulsed with 100μM H3.3K27M$_{26–35}$ peptide. The empty vector (EV) CAR (gray lines) is provided as a negative control; T2 cells pulsed with 100 μM H3.3K27M$_{26–35}$ peptide are provided as a positive control. Shown is the mean 4 h percentage of maximum target cell lysis in triplicate ± SD. Data are representative of two biological replicates.

immunoaffinity purification to capture HLA-A*02:01-bound peptides, followed by a subsequent pan-HLA capture step to purify the remaining HLA class I peptide complexes.

In the HEK293T H3.3 K27M-mutant cell line, we identified a total of 3,880 peptides (8–12 mers) were identified, among which 1,005 peptides were restricted by HLA-A2, while the remaining 2,875 peptides were bound to other HLA class I allotypes (Table S1) (A*03:01, B*07:02, C*03:03). The majority of identified peptides were 9-mers (nonamers), as seen in both HLA-A*02:01 and pan class I eluates (Figures S2A and S2B). The nonamers found in HLA-A2 eluates matched the canonical binding motif for HLA-A*02:01 allele (Figure S2C), while the pan class

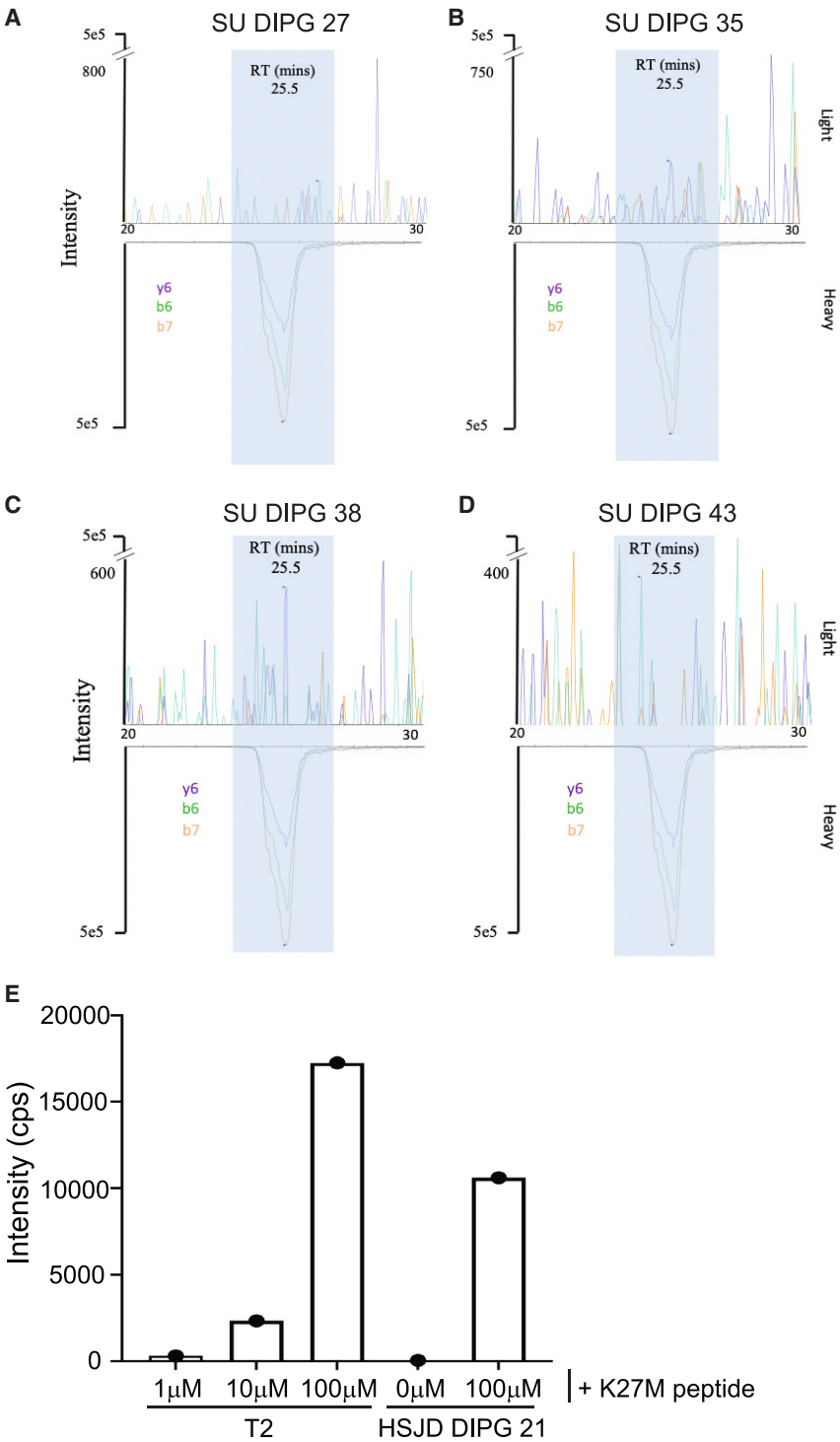

Figure 4. MRM transition profiles reveal absence of the HLA-A*02:01-restricted neopeptide RMSAPSTGGV in DIPG cell lines

LC-MRM was used to detect presence or absence of HLA-A*02:01 restricted neopeptide H3.3K27M$_{26–35}$ peptide, RMSAPSTGGV (native and oxidised version) using three transitions with specific ions indicated. Representative MRM traces for endogenous/light (L) peptide (top) and spiked in heavy (H) peptide (bottom). (A–D) Only the heavy labeled native peptide was detected across the 4 DIPG cell line samples. (E) Quantification of cell surface H3.3K27M$_{26–35}$ peptide eluted from DIPG and T2 cell lines, with or without peptide pulsing, demonstrate no endogenous expression observed in HSJD DIPG 21. Combined peak area is the sum of the peak areas for all transitions monitored.

I motif was predominately composed of a mixture of HLA-A*03:01 and HLA-B*07:02 peptides (Figure S2D).

However, once again, the previously reported HLA-A*02:01 neoepitope, RMSAPSTGGV, was not detected in the mutant HEK293T H3.3K27M protein eluates, despite identifying a total of 11 pHLAs from this protein (Figure 5A). It is worth noting that six of these peptides have been previously reported as HLA-A*02:01 binders in the immune epitope database,[11] which indicates that antigen processing of H3.3 is indeed occurring.

We made a significant discovery of a novel 11mer peptide (RMSAPSTGGVK) encompassing the K27M mutation, which was confidently identified in the pan HLA class I eluate (Figure 5B). This neopeptide sequence matched the binding motif of the endogenous HLA-A*03:01 allotype in the HEK293T cell line. Moreover, this unique neoepitope was detected exclusively in the HEK293T H3.3K27M-mutant cells and was absent from the WT cells. Additionally we observed a modified version of the peptide with oxidation of Met at P2 was also detected (Figure 5C). Together, these observations demonstrate that a novel HLA-A*03:01-restricted H3.3K27M$_{26–36}$ peptide is naturally presented by HEK293T cells transfected with the H3.3K27M protein, and strongly suggests that the H3.3K27M$_{26–35}$ peptide is not processed for presentation via HLA-A*02:01.

To further validate this HLA-A*03:01-restricted neopeptide we used a heavy-labelled peptide approach, similar to the one used for the HLA-A*02:01-restricted determinant. The heavy peptide carried a substitution at Pro in position 5 (13C5, 15N1), thereby introducing a 6-Da mass difference. We spiked 50 fM/μL of both HLA-A*02:01 and -A*03:01 heavy peptides into the HLA-A2 (BB7.2) and pan-HLA (W6/32) fractions eluted from HEK293T H3.3K27M-mutant cells, respectively, and acquired the samples on a Q-Exactive Plus LC-MS system.

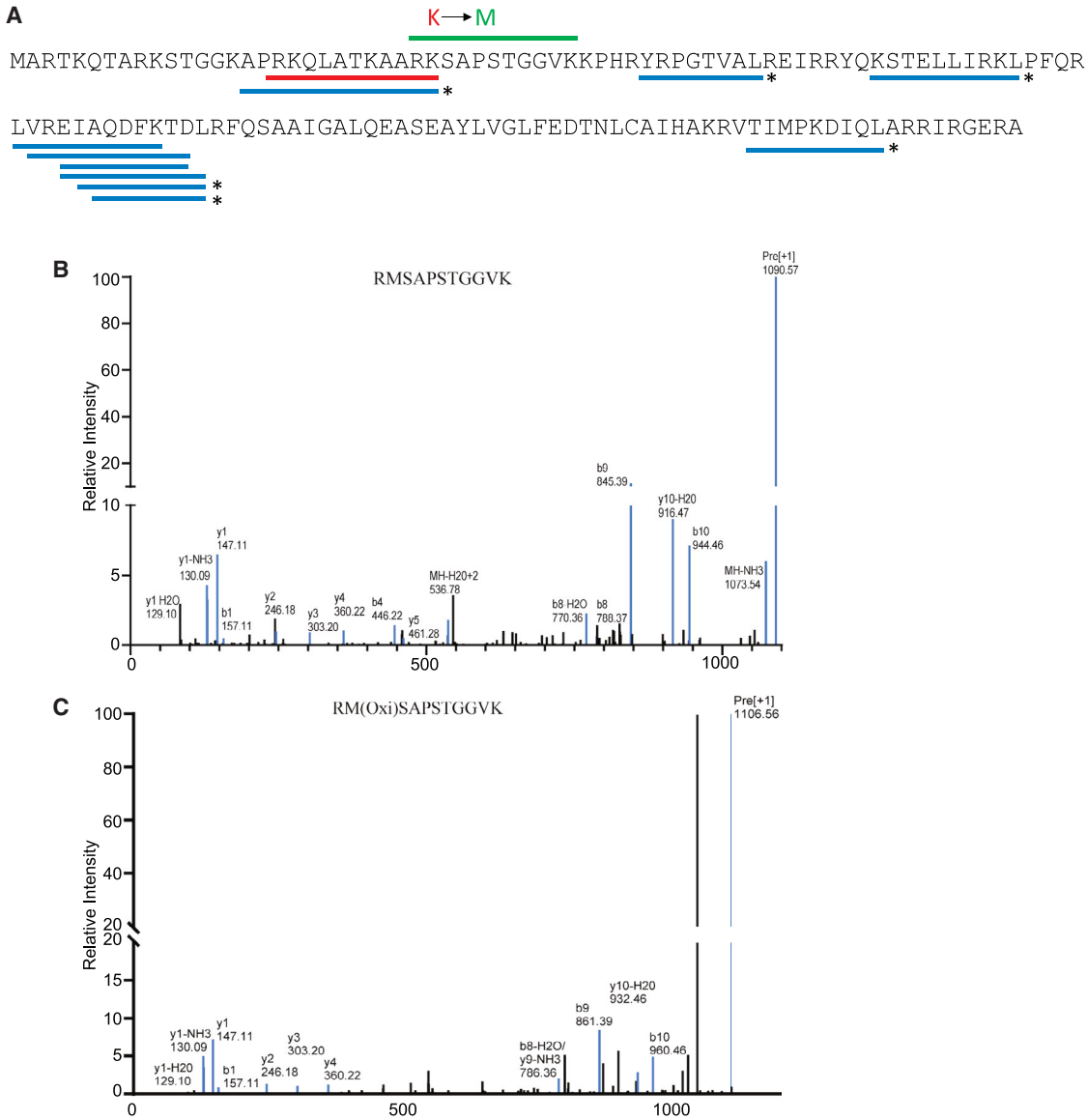

Figure 5. Peptides derived from the H3.3 protein presented by HLA Class I

(A) The HLA class I restricted peptides (underlined in blue) are detected from both WT and H3.3K27M-mutant HEK293T cells, of which six peptides marked with * have been previously reported (and verified in the immune epitope database). An 11-mer peptide including the mutation site, RKQLATKAARK (underlined in red) was detected from pan HLA class I capture from HEK293T WT cells. However, in the K27M-mutant cells, the peptide RMSAPSTGGVK (labeled in green) is detected from pan HLA class I capture instead of WT peptide. The MS/MS fragmentation spectra of the HLA-A*03:01-restricted (B) native version of peptide RMSAPSTGGVK and (C) methionine oxidised version RM(Oxi) SAPSTGGVK of native peptide. X axis represents mass over charge ratio (m/z) and y axis represents the intensity of ions generated from HCD fragmentation of the peptide and sequence ladder of b and y ions identified for the neoepitope RMSAPSTGGVK.

In the HLA-A2 fractions, only the heavy HLA-A*02:01 neoepitope was detected, with no trace of the endogenous peptide. This confirmed the absence of the HLA-A*02:01 neoepitope in the HEK293T model. Importantly, we confidently identified the oxidized version of HLA-A*03:01 neoepitope (RM_{ox}SAPSTGGVK) in the pan-HLA fraction with both the endogenous and heavy peptides co-eluting at 20 min (Figures S3A–S3C). The abundance of the neopeptide in terms of peptide copies/cell was calculated using the intensity of the peptide, and was found to be approximately 6 copies/cell.

To confirm the presentation of the putative HLA-A*03:01-restricted neoepitope (RMSAPSTGGVK), we needed to investigate its presence in a monoallelic system. For this purpose, we generated a CIR HLA-A*03:01 cell line expressing high levels of both HLA-A3 and H3.3K27M-mutant histone (Figure S4). Cell-surface

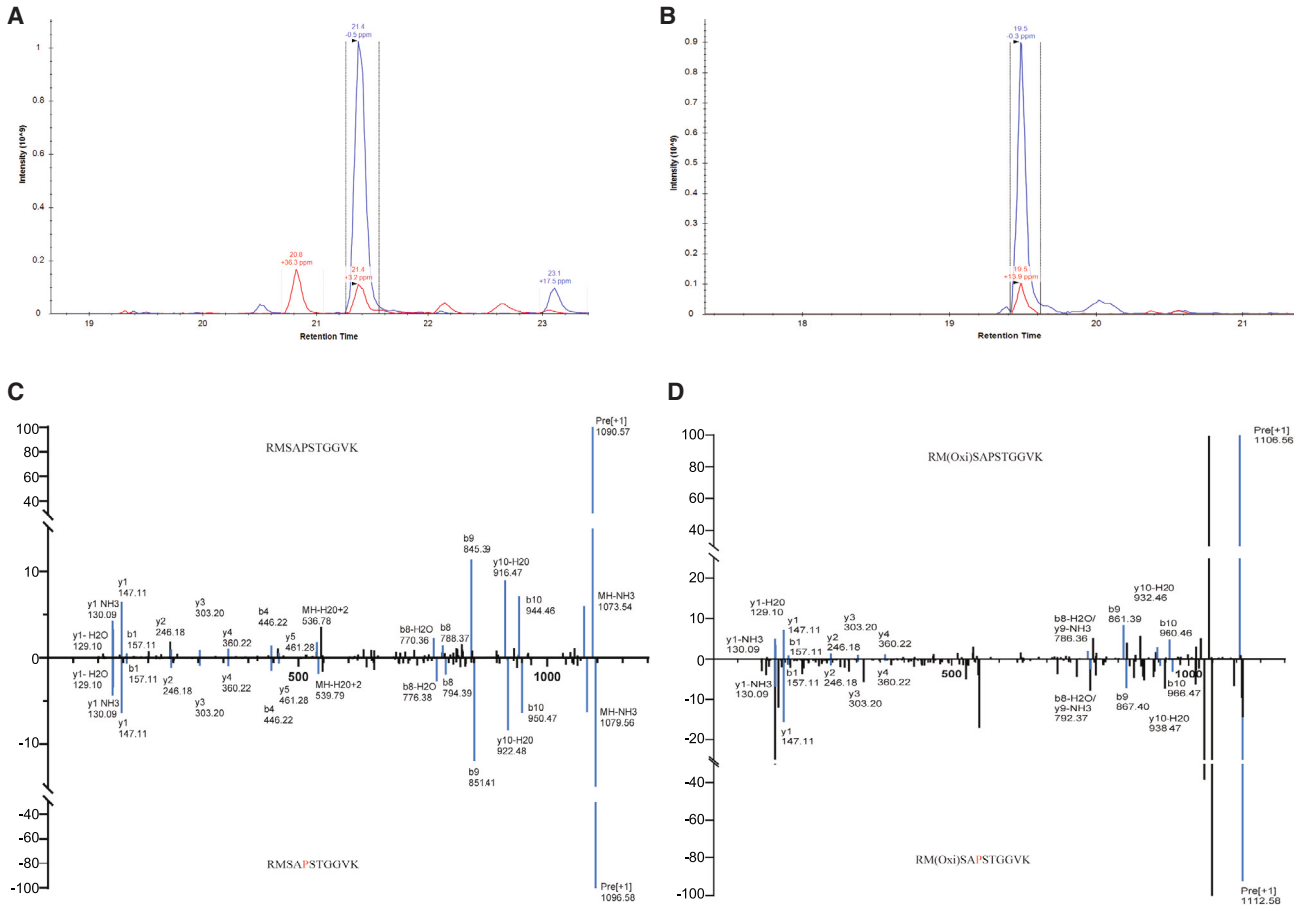

Figure 6. MS/MS identification of HLA-A*03:01-restricted H3.3K27M-mutant peptide RMSAPSTGGVK from HLA elutions

Both peptide versions (A) modified and (B) native were identified in C1R.A*03:01/H3.3K27M cells. Extracted ion chromatograms (XICs) of precursors indicate (A) co-elution of modified peptide RMoxSAPSTGGVK both the heavy (blue) and the endogenous (red) at 19.5 min and (B) co-elution of native peptide RMSAPSTGGVK both the heavy (blue) and the endogenous (red) at 21.4 min. (C) Representative MS/MS fragmentation spectra of HLA-A*03:01-restricted RMSAPSTGGVK peptide with spectra of endogenous peptide (upper) and synthetic heavy labeled peptide (mirror image below) with all b and y ions. The x axis represents mass over charge ratio (*m/z*) and y axis representing the intensity of peptides. (D) Representative MS/MS fragmentation spectra of HLA-A*03:01-restricted oxidised RM(Ox)SAPSTGGVK peptide with spectra of endogenous peptide (upper) and synthetic heavy labeled peptide (mirror image below) with all b and y ions. X axis represents mass over charge ratio (m/z) and y axis representing the intensity of peptides.

expression of HLA-A*03:01 was confirmed using flow cytometry (Figure S4A) and mutant H3.3K27M expression was confirmed by Western blot using an anti-hemagglutinin (HA) tag antibody (Figure S4B).

We conducted immunoaffinity purification to capture HLA-A*03:01-bound peptides (clone GAPA3) from CIR HLA-A*03:01 H3.3K27M cells and immunopeptidomics to confirm the presentation of this neopeptide in the MHC complex. In total, we identified 9,935 HLA-A*03:01 peptides, with the majority being 9mers, followed by 10mers and 11mers (Figure S5). The presence of both the native and modified versions of the HLA-A*03-restricted neopeptide was verified at the MS1 and MS/MS level using the heavy peptide standard. Both native RMSAPSTGGVK and oxidized peptides were detected coeluting with the heavy peptide standards (Figures 6A and 6B). The fragmentation spectra of the endogenous native peptide matched those of the synthetic heavy peptides (Figure 6C) and oxidized peptide (Figure 6D).

Concurrently, we performed similar experiments in a C1R cell line expressing HLA-A*02:01 and H3.3 K27M-mutant protein (Figures S6A–S6D). The peptides identified from this cell line followed the canonical HLA A*02:01 length distribution (with majority of the peptides being nonamers) and motif (Figures S7A and S7B). We also conducted experiments to identify the A2-restricted neopeptide using data-dependent acquisition (DDA) or MRM approaches, but in both cases, no endogenous peptide was detected and only the heavy peptide were identified (Fig-ure S7C).

Our investigations on both the monoallelic HLA-A*03:01 and HLA-A*02:01 systems confirm the presentation of the putative HLA-A*

03:01-restricted neopepitope (RMSAPSTGGVK), while the HLA-A*02:01-restricted neoepitope remains undetected, shedding light on the differential peptide processing and presentation pathways in these cellular contexts.

DISCUSSION

We have previously generated a high-affinity novel scFv antibody binder targeting the HLA-A*02:01 bound to a 10mer peptide encompassing an H3.3K27M mutation,[9] and in this study we observed A615-tetramer binding to T2 cells loaded with titrated H3.3K27M peptide. However, the same H3.3K27M-HLA-A*02:01-specific A615-tetramer failed to recognize the endogenously presented H3.3K27M peptide on the surface of HLA-A*02:01$^+$ DIPG targets. Even when the HSJD DIPG 21 target cells, used in a previous study,[6] were pulsed with an excessive amount of peptide, which induced weak tetramer binding, the A615 CAR T cells did not exhibit a functional cytotoxic response.

The A615 H3.3K27M-specific CAR is functional and we have previously reported the structure of the T cell-target cell immune synapse.[9] While we acknowledge the ability for CARs to recognize peptide:HLA requires a greater antigen density compared to native TCR recognition of peptide/HLA,[12,13] very recently, Willimsky, Immisch et al.[14] demonstrated the same lack of reactivity to H3.3 K27M in a TCR system, and a total lack of responsiveness to DIPG targets using the previously published TCR 1H5 raised against the same peptide antigen. Our study further confirm these findings, and provides evidence that antigen processing of H3.3K27M is responsible for the lack of cell-surface antigen presentation.

In the present study, there were no observations of any reactivity to DIPG cells, either naturally expressing or when exogenously loaded with the mutant H3.3K27M peptide. Unfortunately, both our study and this recent publication[14] are in direct contrast with Chheda et al.,[6] who reported cytotoxic responses induced by the 1H5 TCR toward DIPG cells that were endogenously H3.3K27M mutated. Notably, the study by Chheda et al.[6] that used mass spectrometry to detect H3.3K27M peptide, detected this peptide (albeit at low levels) in U87 cell lines transfected to over-express H3.3K27M, rather than endogenous HLA-A*02:01$^+$ DIPG lines that were H3.3K27M mutated. Recently, the same group responded with a letter presenting modest cytotoxicity data of HSJD DIPG 17 cells being killed by the same TCR-expressing T cells.[15] In contrast, we were unable to detect tetramer binding to any HLA-A*02:01$^+$ DIPG target cells (including HSJD DIPG 17) containing the K27M mutation, either H3.3 or H3.1, nor any functional recognition, even when pulsed with high concentrations of exogenous K27M peptide (Figure 3). Regarding the K27M peptide presentation, while we acknowledge that the "absence of evidence," is not the "evidence of absence" in relation to peptide presentation, our sensitive immunopeptidomics and mass spectrometry failed to detect the HLA-A*02:01 restricted H3.3K27M$_{26–35}$, RMSAPSTGGV neopeptide using DDA methods, as well as sensitive and targeted MRM assays. However, we did identify several non-mutation-containing peptides derived from H3.3, as well as a novel HLA-A*03-restricted 11mer neopeptide (H3.3K27M$_{26–36}$, RMSAPSTGGVK). That the HLA-A*03-derived K27M-mutant protein is degraded and can be presented at the cell surface, demonstrates that the protein containing the K27M mutation can be processed and presented by HLA, and it is not a defect in protein processing that is preventing the peptide from being displayed.

The lack of presentation of the HLA-A2*02:01-derived K27M$_{26–35}$-mutant peptide suggests that this neopepitope is not processed for presentation. Of note, both HSJD DIPG 21 and HSJD DIPG 17 cells have previously been shown to be efficiently killed by TCR-transduced cells in *in vitro* assays and *in vivo* mouse models.[6] This finding may have implications for the interpretation of clinical trials targeting the H3.3K27M mutation in DMG, including a 19-patient study testing a K27M vaccine approach, which has reported an improvement in patient overall survival. However, in this study there was an association between H3.3K27M-reactive T cell expansion and patient outcomes.[8,16] So while this trial reported H3.3K27M-specific T cell responses, as detected using mass cytometry,[8] poor peptide presentation by DMG tumors is unlikely to result in H3.3K27M antigen-specific tumor regression. Having said that, we cannot rule out that other factors, such as ionizing radiation and chemotherapy, may induce stress in the DMG cells and may alter epitope presentation.

In summary, our study using patient-derived DMG models to demonstrated that the H3.3 K27M$_{26–35}$ peptide was not presented sufficiently by HLA-A*02:01 to elicit a meaningful T cell response. Notably, the INTERCEPT-H3 clinical trial (NCT04808245) exploiting a longer H3.3K27M peptide does not require HLA-A*02:01 positivity as an inclusion criterion. Identifying and evaluating less common HLA alleles capable of presenting neoepitope peptides encompassing the K27M mutation may enhance the therapeutic potential of targeting the K27M mutation in the future.

The unique HLA-A3 peptide identified warrants further exploration and may provide some hope for a peptide MHC-targeted therapeutic strategy in the future. Considering the large investment in vaccine and cell-based therapies targeting H3.3K27M$_{26–35}$-HLA-A*02:01, our findings hold clinical significance and are likely to benefit the field. This particular patient cohort, which is in need of new therapies, is especially vulnerable, and we urge further research to identify highly immunogenic targets for translation into clinical practice.

MATERIALS AND METHODS

Cell culture

Patient-derived glioma cells were generated as previously described and were mycoplasma free and authenticity was validated though short tandem repeat fingerprinting of the cells.[17,18] DIPG cell lines were generous gifts from Prof Michelle Monje, Prof Angel Carcaboso, Prof Hideho Okada, and Dr Jason Cain. DIPG models were passaged every 1–2 weeks in working serum free medium (1:1 Neurobasal-A Medium and D-MEM/F-12, Invitrogen) supplemented with B27 (Invitrogen), fibroblast growth factor, epidermal growth factor, platelet-derived growth factor (PDGF)-AA, PDGF-BB (Shenandoah Biotechnology), and heparin (StemCell Technologies).

T2 cells and C1R transfectants were cultured in RF-10 (RPMI-1640 (Gibco) supplemented with 10% fetal calf serum (FCS; Sigma), 1 mM/L sodium pyruvate, 2 mM/L glutamine, 0.1 mM/L nonessential amino acids, 100 U/mL penicillin-streptomycin, and 20 mM/L HEPES [all sourced from Gibco]). Class I reduced (C1R) parental cell line was transfected with a bicistronic construct expressing A*02:01 followed by T2A peptide and H3.3K27M protein and cultured in RF-10 supplemented with G-418 (0.5 mg/mL, Roche). All other cells lines were cultured in DM-10 (DMEM supplemented with 10% FCS [Sigma], 2 mM/L glutamine [Gibco], and 100 U/mL penicillin-streptomycin [Gibco]). Cells were maintained at 37°C, 5% CO_2.

T cells were cultured daily at 0.5×10^6 cells/mL in T cell media, RPMI-1640 (Gibco) supplemented with 10% FCS (Gibco), 1 mM/L sodium pyruvate (Gibco), 2 mM/L glutamine (Gibco), 0.1 mM/L nonessential amino acids (Gibco), 50 μM β-mercaptoethanol (Sigma), and rhIL-2 (Peprotech, #200-02) at 100 IU/mL.

Flow cytometry

HLA-A*02:01 expression was confirmed before each experiment with flow cytometry using an anti-HLA-A*02:01 (BB7.2) antibody (BD Pharmingen, #558570).

HLA class I expression was confirmed before each experiment and measured using flow cytometry. Surface antibody labeling used hybridoma supernatants for anti-HLA-A2 (BB7.2[19]) (BD Pharmingen, #558570), as well as pan-HLA class I (W6/32[20,21]). The level of expression of H3.3K27M in HEK293T-mutant cell lines was examined by intracellular staining of the FLAG-tagged H3.3K27M protein using flow cytometry, as described previously.[22]

C1R parental cell line was transfected with a bicistronic construct expressing A*02:01 followed by T2A peptide and H3.3K27M protein. The construct also expressed dsRED allowing sorting of cells expressing high levels of both H3.3K27M protein and HLA-A*02:01 using an Influx sorter (BD).

The C1R A*03:01 cell line was transfected with a construct generated to express HA tag at the C-terminus of the H3.3 K27M-mutant histone protein. HLA-A*03:01 surface expression was monitored by staining using hybridoma supernatants for anti-HLA-A3 (GAPA3)[23] (HB-122) (ATCC).

Western blotting

The level of expression of the H3.3K27M-mutant histone protein in the C1R A*03:01 cell line was confirmed by western blot using an anti-HA tag antibody 3F10 rat monoclonal (Merck) used at 1:5,000, followed by secondary antibody (goat anti-rat-IgG-HRP) used in 1:10,000 dilution, and developed using horseradish peroxidase. The membrane was scanned with a ChemiDoc Touch Imaging System (Biorad), using Western Lightning Plus-ECL Enhanced Chemiluminescence reagent (PerkinElmer). Image was visualized using the Bio-rad ImageLab Software (v5.2.1) in combination with ImageJ (v1.5i).

Mice

All mice used were 6–8 week old WT female C57Bl/6 mice, sourced from the WEHI animal facility. They were bred and maintained under WEHI approved, specific-pathogen free conditions in the WEHI animal facilities. All experiments were performed under the approval of the WEHI Animal Ethics Committee (#2019.020).

Generation of CAR T cells

Briefly, HEK293T cells were transfected using FuGENE-6 kit (Catalog Number E269A, LOT0000275467, 2019-05-02 Promega) with gag/pol packaging vector, ECO mouse trophic envelope vector, and transfer vector encoding the second-generation CD28z CAR cDNA. T cells were isolated from WT C57Bl/6 mouse lymph nodes by positive selection using either EasySep Mouse positive $CD8^+$ T cell isolation kit (StemCell Technologies) or EasySep Mouse positive $CD4^+$ T cell isolation kit (StemCell Technologies). T cells were then activated using aCD3/CD28 Dynabead (Invitrogen) and transduced with retrovirus on Retronectin (Takeda) coated plates and incubated at 37°C, 5% CO_2. Cells were generally assayed 7–10 days after transduction and adjusted for myc/mCherry transduction efficiencies, for functional assessment. Cell-surface CAR expression was assessed using flow cytometry by labeling with anti-MYC antibody (Clone 9B11, Cell Signaling) at 4°C for 45 min and detection of intracellular mCherry expression, as previously described.[9]

Chromium release assay

Cytotoxicity was examined by labeling the target cells with 100 mCi ^{51}Cr for 1 h at 37°C in T cell media, before excess ^{51}Cr was washed off and target cells cultured at 1×10^4/well in a 96-well plate. CAR T cells were then added at varying effector:target ratios. The plate was incubated at 37°C, 5% CO_2 for 4 h and supernatant harvested to a fresh plate. ^{51}Cr levels in supernatant was read using a β-counter (Luminescence Counter, PerkinElmer) and the percentage of lysis calculated using the following formula: [(experimental counts/minute – spontaneous counts/minute)/(total counts/minute - spontaneous counts/minute)] × 100. The level of ^{51}Cr release from targets alone did not exceed 10% of the total ^{51}Cr release from targets lysed with 1% Triton X-100 to determine maximal lysis, and results are shown as the percentage of cytotoxicity.

Purification of pHLA complexes from H3.3K27M transfected cell lines

HEK293T H3.3 WT and HEK293T H3.3K27M-mutant cells (6×10^8 cells per pellet) and H3.3K27M transfected C1R HLA-A*02:01 and C1R HLA-A*03:01 cells (1×10^9 cells per pellet) were interrogated by immunopeptidomics using previously published methods.[24,25] Briefly, frozen cell pellets were pulverized using a cryogenic mill and solubilized material passed through a PAS pre-column, followed by serial affinity capture columns. For HEK293T cell lines, the lysate was first passed through a BB7.2 column (to pull down HLA-A*02:01 complexes) followed by a W6/32 column (to pull down remaining HLA-A*03:01, B*07:02, and C*03:03 complexes). For the C1R HLA-A*02:01 and C1R HLA-A*03:01 H3.3K27M transfected cell lines, lysates were passed sequentially through BB7.2 and GAPA3

(to pull down HLA-A*03:01 complexes) column, respectively, followed by a W6/32 column (to pull down remaining HLA I complexes). Bound complexes were eluted from the individual columns using 10% acetic acid. Eluates of all transfected cell lines were fractionated by reverse phase high-performance liquid chromatography (HPLC). A total of 43 peptide-containing fractions were collected, vacuum concentrated, and concatenated into three peptide-containing pools for each immunoprecipitate and were analyzed by liquid chromatography tandem mass spectrometry (LC-MS/MS) on a QE Plus Orbitrap (for HEK293T WT, HEK293T-mutant, transfected C1R HLA-A*03:01) or Bruker TimsTOF (for transfected C1R HLA-A*02:01) LC-MS.

Purification of HLA-peptide complexes from DIPG cell lines

Small-scale immunoaffinity purifications were performed for the four DIPG cell lines (SU DIPG 27, SU DIPG 35, SU DIPG 38, and SU DIPG 43) as described.[26] Briefly, cells (approximately 2×10^7) were lysed at 4°C for 1 h and solubilized pHLA complexes were captured using BB7.2 followed by W6/32 resin. Bound pHLA complexes were eluted using 10% acetic acid and the eluate passed through a 5 kDa molecular weight cut off filter (Amicon, Sigma-Aldrich). The filtrate was concentrated and desalted by C18 stage tips (Omix, Agilent). Samples were interrogated by LC-MS/MS using a Q-Exactive Plus (QE Plus) mass spectrometer (Thermo Scientific) and subsequently interrogated for specific peptides using targeted LC-MRM approaches.[27,28]

Analysis of HLA class I-bound peptides by LC-MS/MS

The Q-Enactive Plus Hybrid Quadrupole Orbitrap (Thermo Fisher Scientific) LC-MS was run in DDA mode coupled online to an RSLC nano HPLC (ultimate 3000 UHPLC, ThermoFisher Scientific), as previously described.[29] The transfected C1R HLA-A*02:01 fractions were acquired using a Bruker TimsTOF PRO hybrid trapped ion mobility-quadrupole time of flight MS (Bruker Daltonics) coupled with a nanoElute liquid chromatography system. Sample was loaded directly onto the C_{18} analytical column (Aurora, IonOpticks) of 1.6-μm particle size and 75 μm × 25 cm and 120 Å using a 20-min linear gradient of buffer A1 (2% ACN, 0.1% FA). Peptides were eluted from the column with flow rate set to 400 nL/min, by a linear stepwise gradient of buffer B1 (100% ACN, 0.1% FA) against buffer A1 initially to 17% over 60 min, then to 25% over 30 min, and 37% over 10 min, followed by rapid rise to 95% over 10 min. DDA was performed with following settings: *mz* range, 100–1700 *mz*; capillary voltage,1,600 V; target intensity, 30,000; and TIMS ramp, 0.60–1.60 Vs./cm^2 for 166 ms.

Synthetic peptides

The previously reported HLA-A*02:01 restricted H3.3K27M$_{26–35}$ (RMSAPSTGGV), gp100(IMDQVPFSV) peptides, and stable isotope-labeled synthetic H3.3K27M peptides ^{26}RMSAPSTGGV^{35} and ^{26}RMSAPSTGGVK^{36} incorporating a heavy Proline at P5 (13C5, 15N1) were synthesized by Mimotopes at more than 95% purity as indicated by analytic HPLC and MS analyses. Peptide stocks were dissolved in DMSO (Sigma-Aldrich) at a concentration of 10 mg/mL and stored at −80°C until use. For peptide loading, T2 and HEK293T cells were incubated overnight with 100 mM peptide at 26°C, 5% CO_2.[30]

MRM and MRM-HR quantification of HLA bound peptides

The HLA-A*02:01-positive DIPG cell line eluates were spiked with the H3.3K27M$_{26–35}$ heavy peptide. Samples were assessed for the presence of peptide by MRM using SCIEX QTRAP 6500+ mass spectrometer, equipped with an on-line Ekspert nanoLC 415 (Eksigent) autosampler using Analyst 1.6 (SCIEX) software, as previously described.[27] The eluates of peptide pulsed T2 cells, SU DIPG 21 cells, and SU DIPG 36 cells were spiked with the H3.3K27M$_{26–35}$ heavy peptide and assessed for the presence of endogenous peptide by MRM-HR[28] using SCIEX 7600 mass spectrometer. MRM and MRM-HR data were visualized on Skyline software 64-bit v4.1.0 (MacCoss Laboratory).

Mass spectrometry data analysis

All MS/MS raw files were exported and analyzed using Peaks software (Bioinformatics Solutions) searching against the human proteome (Uniprot 15/06/2017; 20,182 entries) wherein the H3.3K27M protein sequence was appended. For immunopeptidomic data analysis, a 5% false discovery rate cut off was applied. MS/MS data from pPeaks searches (peptide.csv) for each cell line is provided in Tables S4, S5, and S6. All data are available upon request.

Statistical analysis

Statistical analyses were performed using GraphPad Prism 8 software. Statistical tests applied include Student t-test and two-way ANOVA with *post hoc* analysis using Tukey's multiple comparisons. Asterisks within figures refer to statistical difference between test and control groups, p values and the number of replicate experiments performed to derive the data are indicated in the figure legends.

DATA AND CODE AVAILABILITY

The mass spectrometry proteomics data have been deposited to the ProteomeXchange Consortium (http://proteomecentral.proteomexchange.org) via the PRIDE partner repository[31] with the dataset identifier PXD038371. (Project DOI: 10.6019/PXD038271) [Username: reviewer_pxd038271@ebi.ac.uk; password: 7U5pG9x9]). All data available on request.

SUPPLEMENTAL INFORMATION

Supplemental information can be found online at https://doi.org/10.1016/j.omto.2023.08.005.

ACKNOWLEDGMENTS

We acknowledge Myrio Therapeutics for generating the HLA-A*02:01-restricted K27M neoepitope binder.[9] We are very grateful for the generosity of Prof Michelle Monje (Stanford), Prof Angel Carcaboso (Hospital Sant Joan de Deu, (HSJD) (Barcelona), Prof Hideho Okada (University of California, San Francisco), Dr Jason Cain (Hudson Institute), Prof Andrew Brooks (Doherty Institute), and Assoc. Prof. Lee Wong (Monash University) for providing cell lines and reagents. We are grateful to Prof Okada for excellent and generous discussions of our work. Computational resources were supported by the R@CMon/Monash Node of the NeCTAR Research Cloud, an initiative of the Australian Government's Super Science Scheme and the

Education Investment Fund. We acknowledge the Monash Proteomics & Metabolomics Facility and FlowCore, for the provision of instrumentation, training, and technical support.

We thank the following for financial support: Australian National Health and Medical Research (NHMRC), Cancer Australia (APP 1164657), Robert Connor Dawes Foundation, Isabella and Marcus Foundation, and the Mark Hughes Foundation. This was made possible in part and financially supported through the author's membership of the Brain Cancer Center. S.S.W. is funded by the Matthew Rathbone Clinical Research Fellowship, My Room Children's Cancer Charity. M.R.J. is supported by an NHMRC Investigator Grant (APP11 72858). R.S.C. was funded by Cure Brain Cancer Foundation Fellowship. A.W.P. is supported by an NHMRC Principal Research Fellowship (APP1137739).

We acknowledge this work was performed and reported on lands traditionally owned by the Wurundjeri people of the Kulin Nation.

AUTHOR CONTRIBUTIONS

M.R.J., A.W.P., and R.C. conceived and designed the project, all authors conducted experiments and analyzed data; S.S.W., K.P., A.W.P., and M.R.J. wrote the manuscript. The manuscript was edited and reviewed by all the authors.

DECLARATION OF INTERESTS

A.W.P. is a member of the scientific advisory board (SAB) of Bioinformatic Solutions Inc. (Canada), is a shareholder and SAB member of Evaxion Biotech (Denmark), and a co-founder of Resseptor Therapeutics (Melbourne, Australia). No entity had any influence on this publication. The other authors have no conflicts to declare.

REFERENCES

1. Vanan, M.I., and Eisenstat, D.D. (2015). DIPG in Children - What Can We Learn from the Past? Front. Oncol. *5*, 237. https://doi.org/10.3389/fonc.2015.00237.

2. Sturm, D., Bender, S., Jones, D.T.W., Lichter, P., Grill, J., Becher, O., Hawkins, C., Majewski, J., Jones, C., Costello, J.F., et al. (2014). Paediatric and adult glioblastoma: multiform (epi)genomic culprits emerge. Nat. Rev. Cancer *14*, 92–107. https://doi.org/10.1038/nrc3655.

3. Khuong-Quang, D.A., Buczkowicz, P., Rakopoulos, P., Liu, X.Y., Fontebasso, A.M., Bouffet, E., Bartels, U., Albrecht, S., Schwartzentruber, J., Letourneau, L., et al. (2012). K27M mutation in histone H3.3 defines clinically and biologically distinct subgroups of pediatric diffuse intrinsic pontine gliomas. Acta Neuropathol. *124*, 439–447. https://doi.org/10.1007/s00401-012-0998-0.

4. Wu, G., Diaz, A.K., Paugh, B.S., Rankin, S.L., Ju, B., Li, Y., Zhu, X., Qu, C., Chen, X., Zhang, J., et al. (2014). The genomic landscape of diffuse intrinsic pontine glioma and pediatric non-brainstem high-grade glioma. Nat. Genet. *46*, 444–450. https://doi.org/10.1038/ng.2938.

5. Buczkowicz, P., and Hawkins, C. (2015). Pathology, Molecular Genetics, and Epigenetics of Diffuse Intrinsic Pontine Glioma. Front. Oncol. *5*, 147. https://doi.org/10.3389/fonc.2015.00147.

6. Chheda, Z.S., Kohanbash, G., Okada, K., Jahan, N., Sidney, J., Pecoraro, M., Yang, X., Carrera, D.A., Downey, K.M., Shrivastav, S., et al. (2018). Novel and shared neoantigen derived from histone 3 variant H3.3K27M mutation for glioma T cell therapy. J. Exp. Med. *215*, 141–157. https://doi.org/10.1084/jem.20171046.

7. Leidner, R., Sanjuan Silva, N., Huang, H., Sprott, D., Zheng, C., Shih, Y.P., Leung, A., Payne, R., Sutcliffe, K., Cramer, J., et al. (2022). Neoantigen T-Cell Receptor Gene Therapy in Pancreatic Cancer. N. Engl. J. Med. *386*, 2112–2119. https://doi.org/10.1056/NEJMoa2119662.

8. Mueller, S., Taitt, J.M., Villanueva-Meyer, J.E., Bonner, E.R., Nejo, T., Lulla, R.R., Goldman, S., Banerjee, A., Chi, S.N., Whipple, N.S., et al. (2020). Mass cytometry detects H3.3K27M-specific vaccine responses in diffuse midline glioma. J. Clin. Invest. *130*, 6325–6337. https://doi.org/10.1172/JCI140378.

9. Wang, S.S., Luong, K., Gracey, F.M., Jabar, S., McColl, B., Cross, R.S., and Jenkins, M.R. (2021). A Novel Peptide-MHC Targeted Chimeric Antigen Receptor T Cell Forms a T Cell-like Immune Synapse. Biomedicines *9*, 1875. https://doi.org/10.3390/biomedicines9121875.

10. Dellgren, C., Nehlin, J.O., and Barington, T. (2015). Cell surface expression level variation between two common Human Leukocyte Antigen alleles, HLA-A2 and HLA-B8, is dependent on the structure of the C terminal part of the alpha 2 and the alpha 3 domains. PLoS One *10*, e0135385. https://doi.org/10.1371/journal.pone.0135385.

11. Vita, R., Mahajan, S., Overton, J.A., Dhanda, S.K., Martini, S., Cantrell, J.R., Wheeler, D.K., Sette, A., and Peters, B. (2019). The Immune Epitope Database (IEDB): 2018 update. Nucleic Acids Res. *47*. D339–d343. https://doi.org/10.1093/nar/gky1006.

12. Majzner, R.G., Rietberg, S.P., Sotillo, E., Dong, R., Vachharajani, V.T., Labanieh, L., Myklebust, J.H., Kadapakkam, M., Weber, E.W., Tousley, A.M., et al. (2020). Tuning the Antigen Density Requirement for CAR T-cell Activity. Cancer Discov. *10*, 702–723. https://doi.org/10.1158/2159-8290.CD-19-0945.

13. Walker, A.J., Majzner, R.G., Zhang, L., Wanhainen, K., Long, A.H., Nguyen, S.M., Lopomo, P., Vigny, M., Fry, T.J., Orentas, R.J., and Mackall, C.L. (2017). Tumor Antigen and Receptor Densities Regulate Efficacy of a Chimeric Antigen Receptor Targeting Anaplastic Lymphoma Kinase. Mol. Ther. *25*, 2189–2201. https://doi.org/10.1016/j.ymthe.2017.06.008.

14. Immisch, L., Papafotiou, G., Popp, O., Mertins, P., Blankenstein, T., and Willimsky, G. (2022). H3.3K27M mutation is not a suitable target for immunotherapy in HLA-A2(+) patients with diffuse midline glioma. J. Immunother. Cancer *10*, e005535. https://doi.org/10.1136/jitc-2022-005535.

15. Chheda, Z.S., Mueller, S., Hegde, B., Yamamichi, A., Butterfield, L.H., and Okada, H. (2023). Correspondence on 'H3.3K27M mutation is not a suitable target for immunotherapy in HLA-A2+ patients with diffuse midline glioma' by Immisch et al. J. Immunother. Cancer *11*, e006617. https://doi.org/10.1136/jitc-2022-006617.

16. Ochs, K., Ott, M., Bunse, T., Sahm, F., Bunse, L., Deumelandt, K., Sonner, J.K., Keil, M., von Deimling, A., Wick, W., and Platten, M. (2017). K27M-mutant histone-3 as a novel target for glioma immunotherapy. Oncoimmunology *6*, e1328340. ARTN e1328340. https://doi.org/10.1080/2162402X.2017.1328340.

17. Lin, G.L., and Monje, M. (2017). A Protocol for Rapid Post-mortem Cell Culture of Diffuse Intrinsic Pontine Glioma (DIPG). J. Vis. Exp. https://doi.org/10.3791/55360.

18. Mount, C.W., Majzner, R.G., Sundaresh, S., Arnold, E.P., Kadapakkam, M., Haile, S., Labanieh, L., Hulleman, E., Woo, P.J., Rietberg, S.P., et al. (2018). Potent antitumor efficacy of anti-GD2 CAR T cells in H3-K27M(+) diffuse midline gliomas. Nat. Med. *24*, 572–579. https://doi.org/10.1038/s41591-018-0006-x.

19. Parham, P., and Brodsky, F.M. (1981). Partial purification and some properties of BB7.2. A cytotoxic monoclonal antibody with specificity for HLA-A2 and a variant of HLA-A28. Hum. Immunol. *3*, 277–299. https://doi.org/10.1016/0198-8859(81)90065-3.

20. Barnstable, C.J., Bodmer, W.F., Brown, G., Galfre, G., Milstein, C., Williams, A.F., and Ziegler, A. (1978). Production of monoclonal antibodies to group A erythrocytes, HLA and other human cell surface antigens-new tools for genetic analysis. Cell *14*, 9–20. https://doi.org/10.1016/0092-8674(78)90296-9.

21. Parham, P., Barnstable, C.J., and Bodmer, W.F. (1979). Use of a monoclonal antibody (W6/32) in structural studies of HLA-A,B,C, antigens. J. Immunol. *123*, 342–349.

22. Gorasia, D.G., Dudek, N.L., Safavi-Hemami, H., Perez, R.A., Schittenhelm, R.B., Saunders, P.M., Wee, S., Mangum, J.E., Hubbard, M.J., and Purcell, A.W. (2016). A prominent role of PDIA6 in processing of misfolded proinsulin. Biochim. Biophys. Acta *1864*, 715–723. https://doi.org/10.1016/j.bbapap.2016.03.002.

23. Berger, A.E., Davis, J.E., and Cresswell, P. (1982). Monoclonal antibody to HLA-A3. Hybridoma *1*, 87–90. https://doi.org/10.1089/hyb.1.1982.1.87.

24. Purcell, A.W., Ramarathinam, S.H., and Ternette, N. (2019). Mass spectrometry-based identification of MHC-bound peptides for immunopeptidomics. Nat. Protoc. *14*, 1687–1707. https://doi.org/10.1038/s41596-019-0133-y.

25. Pandey, K., Mifsud, N.A., Lim Kam Sian, T.C.C., Ayala, R., Ternette, N., Ramarathinam, S.H., and Purcell, A.W. (2020). In-depth mining of the

immunopeptidome of an acute myeloid leukemia cell line using complementary ligand enrichment and data acquisition strategies. Mol. Immunol. *123*, 7–17. https://doi.org/10.1016/j.molimm.2020.04.008.

26. Pandey, K., Ramarathinam, S.H., and Purcell, A.W. (2021). Isolation of HLA Bound Peptides by Immunoaffinity Capture and Identification by Mass Spectrometry. Curr. Protoc. *1*, e92. https://doi.org/10.1002/cpz1.92.

27. Tan, C.T., Croft, N.P., Dudek, N.L., Williamson, N.A., and Purcell, A.W. (2011). Direct quantitation of MHC-bound peptide epitopes by selected reaction monitoring. Proteomics *11*, 2336–2340. https://doi.org/10.1002/pmic.201000531.

28. Sun, R., Hunter, C., Chen, C., Ge, W., Morrice, N., Liang, S., Zhu, T., Yuan, C., Ruan, G., Zhang, Q., et al. (2020). Accelerated Protein Biomarker Discovery from FFPE Tissue Samples Using Single-Shot, Short Gradient Microflow SWATH MS. J. Proteome Res. *19*, 2732–2741. https://doi.org/10.1021/acs.jproteome.9b00671.

29. Habel, J.R., Nguyen, A.T., Rowntree, L.C., Szeto, C., Mifsud, N.A., Clemens, E.B., Loh, L., Chen, W., Rockman, S., Nelson, J., et al. (2022). HLA-A*11:01-restricted CD8+ T cell immunity against influenza A and influenza B viruses in Indigenous and non-Indigenous people. Plos Pathog. *18*, e1010337. https://doi.org/10.1371/journal.ppat.1010337.

30. Luft, T., Rizkalla, M., Tai, T.Y., Chen, Q., MacFarlan, R.I., Davis, I.D., Maraskovsky, E., and Cebon, J. (2001). Exogenous peptides presented by transporter associated with antigen processing (TAP)-deficient and TAP-competent cells: intracellular loading and kinetics of presentation. J. Immunol. *167*, 2529–2537.

31. Perez-Riverol, Y., Bai, J., Bandla, C., García-Seisdedos, D., Hewapathirana, S., Kamatchinathan, S., Kundu, D.J., Prakash, A., Frericks-Zipper, A., Eisenacher, M., et al. (2022). The PRIDE database resources in 2022: a hub for mass spectrometry-based proteomics evidences. Nucleic Acids Res. *50*. D543–d552. https://doi.org/10.1093/nar/gkab1038.